Journal of Constructional Steel Research 183 (2021) 106756

Contents lists available at ScienceDirect

Journal of Constructional Steel Research

Experimental behaviour of non-seismical RWS connections with perforated beams under cyclic actions

Konstantinos Daniel Tsavdaridis [a,*], Chun Kit Lau [b], Andres Alonso-Rodríguez [c]

[a] School of Civil Engineering, Faculty of Engineering and Physical Sciences, University of Leeds, Woodhouse Lane, West Yorkshire, Leeds LS2 9JT, UK
[b] Civil Engineer, Amey Consulting, 22A Atlas Way, Sheffield S4 7QQ, UK
[c] Institute for Risk and Uncertainty, University of Liverpool, Chadwick Building, Liverpool L69 7ZF, UK

ARTICLE INFO

Article history:
Received 4 December 2020
Received in revised form 8 May 2021
Accepted 11 May 2021
Available online 21 May 2021

Keywords:
RWS connections
Cyclic loads
Seismic retrofitting
Cellular beams
Perforated beams

ABSTRACT

The use of perforated (in particular cellular and castellated) beams has become widespread as their manufacturing processes keep minimising wasted material and has become cost-effective by reducing self-weight of steel structures, while allowing for larger clear spans. Although their behaviour to time-invariant vertical loads has been extensively investigated and validated in laboratory setups, their response to reversible actions has not been explored to the same extent. This paper presents results of cyclic load tests of beam-column reduced web section (RWS) connections, considering setups representative of what is observed in low-rise buildings in the UK; a region with sparse seismicity. Results show that RWS connections on these frames can achieve stable hysteresis loops without significant strength degradation, due to the simultaneous occurrence of yielding of the critical cross-section and development of a Vierendeel mechanism on the edges of the perforations (web openings). Also, inelastic action is mostly observed within the beam, thus being successful in protecting the beam-column connection. Performance particularly exceeds what is observed for a benchmarking RBS connection styled according to the same underlying assumptions, hinting that RWS connections could be a more suitable solution for structural retrofitting in regions where seismicity is sparse.

1. Introduction

Structural steel is one of the most cost-effective construction materials. Its low self-weight structural capacity ratio, low variability and high ductility offer builders great flexibility, which makes its use widespread. However, it is also quite demanding on the environment as its manufacture is very energy-intensive, leading to a large ecological footprint. For example, it has been estimated that hot-rolled steel production in China can generate as much as 3 tons of equivalent CO_2 per ton of final manufactured produce [20].

To keep the steel construction industry sustainable, use of steel must be optimised to the greatest extent. Therefore, there is a pressing need to minimise the self-weight of steel structural systems. One of the most promising ways to achieve this outcome is by considering cellular or other perforated beams. Moreover, lighter structures have the tendency to perform really well to earthquake loads as their own weight do not increase forces in the members.

Most of the flexural capacity of a steel cross-section originates in concurrent compression and tension of their flanges, while the shear is mostly carried by its web. As maximum moment and shear demands do not occur at the same locations, particularly for vertical loads; it is a reasonable course of action to weaken the web by providing web openings in it. There is a slight reduction in the flexural resistance, but this can be overcome by savings in self-weight. With advanced manufacturing techniques, waste during fabrication of cellular beams can be minimised, making them more environmentally sustainable. Consequently, there is extensive research on the behaviour of cellular beams to non-reversible loads for a wide range of perforation shapes [9,15,26,30], which has led to design guidelines considering non-dynamic excitations, being among the most representative the ASCE specifications [3]; the P355 guidelines of the UK's Steel Construction Institute [17] and the Design Guide 31 of the American Institute of Steel Construction [11].

At first sight, perforations would compromise the behaviour of frames of cellular beams when subjected to cyclic actions, as moment and shear demands could be large in the same locations along their length. However, it is possible to employ Reduced Web Sections (RWS) connections for developing ways to migrate the inelastic action on a column-beam joint away from the connection end, ensuring that yielding is constrained to the beam. This is done by creating perforations on the beam web that would lead to the development of a Vierendeel yield mechanism, which is known to be reliable for enduring cyclic actions [4,5,8,10,16,19,22,28,31]. This is an alternative to the widely used

* Corresponding author.
E-mail address: k.tsavdaridis@leeds.ac.uk (K.D. Tsavdaridis).

https://doi.org/10.1016/j.jcsr.2021.106756

Reduced Beam Section (RBS) connection [13], which instead considers trimming of flanges for this purpose. However, this course of action is highly disruptive when being executed for retrofitting, as any alteration on a beam flange would require removal of flooring while creating perforations within a beam web could be done easier from the storey below.

This paper explores the suitability of RWS connections for enduring cyclic actions, despite not being detailed for ductile behaviour (via a seismic-resistant design), as it is often the case in countries were seismicity is uncommon. This is done through validation by laboratory testing. Moreover, the testing campaign builds upon previous research that studied the issue through numerical models [26,27]. Results obtained validate the analytical work and show that RWS connections are capable of achieving stable hysteresis cycles, without displaying signs of fragile failure.

2. Behaviour of RWS and RFS beams after yielding

Finite Element Models (FEM) and non-cyclic-load experiments on well-designed perforated beams with circular web openings show that yielding initiates in the vicinity of the opening closest to the beam-column connection (aka low moment side, LMS) in the compression side, at an angle close to 24 degrees from the vertical centreline, as shown in Fig. 1 [31]. Then plasticity spreads along the edge of the perforation until reaching the smallest cross-section. Similarly, other plastic zones develop at the bottom-end and on the edge of the perforation away from the connection, leading to four well-defined plastic hinges, thus conforming the formation of the Vierendeel mechanism. Still, extensive yielding is also observed in the flange and over the critical section (at the crown of the arches defined by half segments of the web openings) indicating that overall yielding of the critical section is also plausible.

Consequently, post-yield behaviour of the RWS connections is governed by two overlapping phenomena, plastification of the reduced cross-section and development of the Vierendeel mechanism that spans across the closest opening to the beam-column connection (LMS). This mechanical setup is desirable when subjected to cyclic actions as it allows for extensive deformation capacity when reversible actions occur, while not-being prone to out-of-plane torsional and buckling instability.

Moreover, the development of the Vierendeel mechanism caps the shear that can develop within the beam, limiting unexpected failure of non-yielding components of the beam-column connection. Thus, it is highly desired for seismic applications, being a specific case the Special Truss Moment Frames [6] which are a mainstream structural solution in steel seismic design [1].

A free body diagram around the perforation (Fig. 1) allows for the establishment of the following relationship between the plastification moment of the critical cross-section and the Vierendeel mechanism moments:

$$M_{tp} \geq \frac{M_p}{2}\left(1+\frac{1}{4}\frac{D}{L-2S-D}\right) \tag{1}$$

where M_{tp} is the Vierendeel mechanism moment, which depends on the bending capacity of the tee sections around the web openings, M_p is the moment capacity of the beam at the critical section, D is the opening diameter, S is the distance between the beam-column connection and the first opening, and L is the beam span up to the critical section. If the relationship in Eq. (1) holds, the flexural capacity of the tee sections is large enough to allow for plastification of the whole cross-section. Otherwise, the Vierendeel mechanism will occur first.

The yield moment capacity of the cross-section is given by the following:

$$M_p = \left(Z-\frac{D^2 t_w}{4}\right) f_y \tag{2}$$

where Z is its section modulus, D the diameter of the web openings (Fig. 1), t_w is the web's thickness and, f_y is the expected yield stress; while the following lower-bound estimate of the Vierendeel moment can be proposed [17]:

$$M_{tp} = Z_{tee} f_y \tag{3}$$

The expected elastoplastic moment capacity of RBS beams is [1]:

$$M_{max} > M_n = \left[Z-2b_e t_f (h-t_f)\right] f_y \tag{4}$$

where b_e is the width of the trimmed section (Fig. 2). Other, less desirable phenomenon that is observed in steel beams is the local buckling of either flanges and webs, and the lateral torsion of flanges. Unlike the full development of the Vierendeel mechanism, local buckling leads to sudden instability and subsequent loss of load-bearing capacity [21]. Its occurrence in RBS connections and solid beams is controlled by limiting the ratios of flange thickness and unsupported height of the web, the ratio of flange thickness and the unsupported length of the flange [1]. These limits preclude its occurrence before achieving storey drift ratios larger than 2% and 4% depending on thresholds being enforced; being the first limit for elements expected to endure moderate ductility demands while the former is for elements capable of high ductility. As RWS connections are still being developed as a structural solution, thresholds that would prevent buckling and torsion of flanges and webs have not been formally established. This study is a first approach at assessing their response experimentally when subjected to cyclic actions, focusing on the deformation thresholds at which stable hysteric behaviour can be reliably expected.

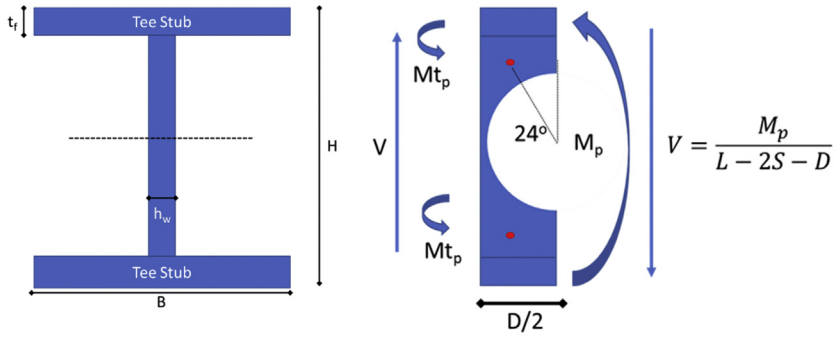

Fig. 1. Vierendeel mechanism.

Fig. 2. Schematic top-view of a RBS beam.

3. Experimental setup

The main purpose of this research programme is to verify through a controlled test the post-yield behaviour of steel frames without specific seismic detailing, i.e., widely used in countries where seismic risk is low. For this task, a frame comprised of a 305 × 127 × 48 UB beam and a 203 × 203 × 71 UC column was considered. It represents in real scale a frame with a beam span of 6m and a story height of 3m, this leads to a beam clear-span depth ratio of 18.6 which is expected in retail stores that require abundant open space [23], particularly in light retail buildings in the UK. Selected beams and columns are equivalent to IPE300 and HE160B standard European steel sections. Openings were cut in the beam web according to the standard cutout process [24,25,29] for perforated beams. Behaviour is expected to be affected slightly by the manufacturing process, therefore results are also representative of behaviour of industrially produced beams.

The test setup was erected in the Heavy Structures George Earle Laboratory in the School of Civil Engineering at the University of Leeds. It represents an internal beam-column connection, as shown in Fig. 3. An actuator applies a load at the midspan on the beam, while the column is fixed at its base and its top is allowed translation and rotation but constrained out-of-plane thus, representing the inflexion point within the second floor. The constrain at the base is provided by 4 M20 (Class 10.9) anchor bolts, double washers and nuts.

Further support was provided at 1750mm away from the column face, corresponding to one-quarter of the clear beam span of the connection being modelled to limit out-of-plane deformation. As a first guideline, design recommendations by AISC were adopted which establish that for beams, lateral buckling and torsion before achieving the full plastic capacity of the beam can be precluded if bracing is provided for at a length lower than the minimum bracing length required for achieving full plastification of the cross-section L_p, which for this case it is 5.2m. This is noticeably larger than what was considered in this test setup. Precisely, one of the outcomes of this testing campaign is verifying if these limits are valid for RWS connections.

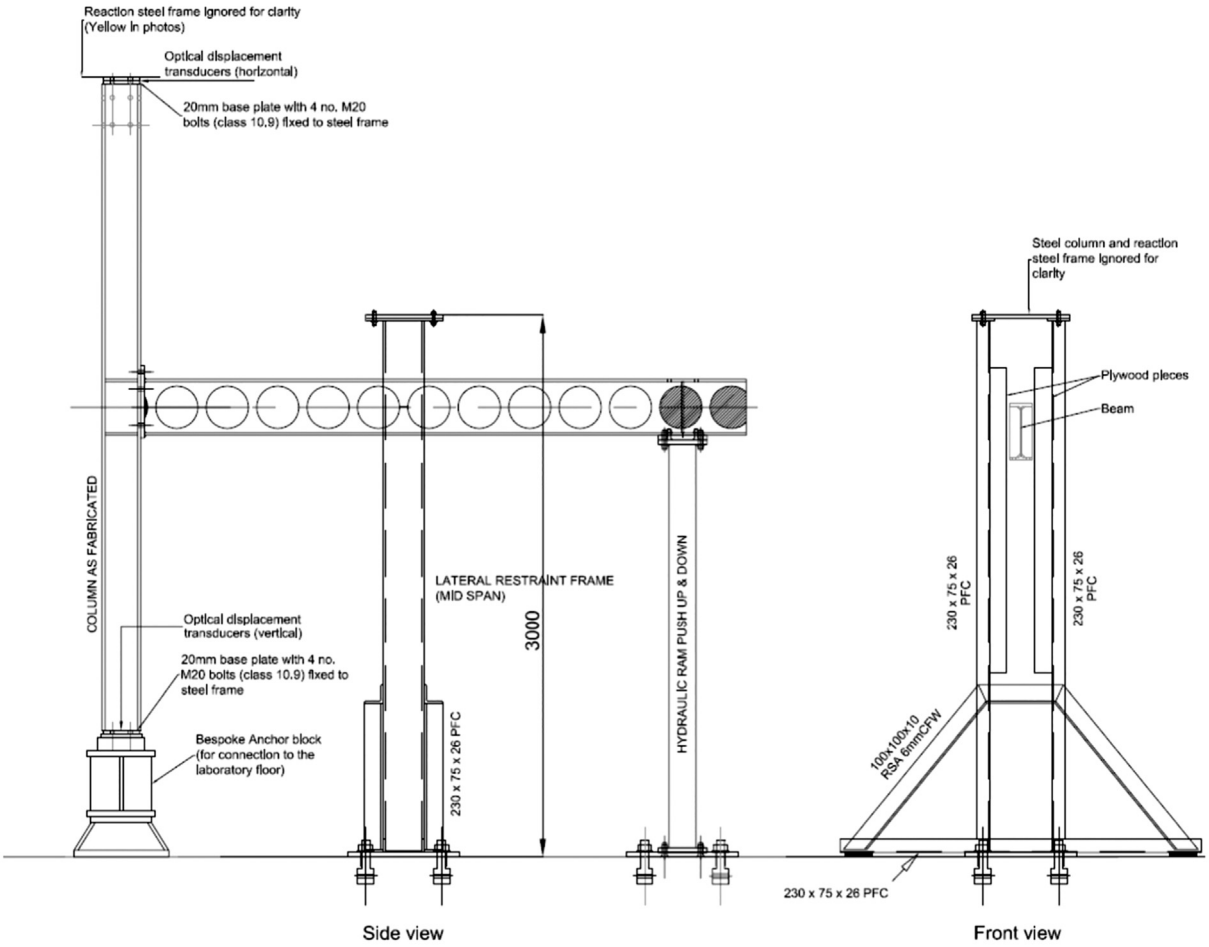

Fig. 3. Test setup.

The main control of the test is through displacement and load monitoring at the beam inflexion point, where a vertical load is applied. Further displacement monitoring is done by optical transducers which record vertical displacements at the column base and horizontal displacements at its top end (Fig. 3). This way column base uplift and column drift can be properly accounted for. 24 supplemental LVDTs were placed along the beam and column flanges to assess their local deflections as shown in Figs. 4 and 5. Strains were monitored trough uniaxial strain gauges (Fig. 6) placed mostly on the column flanges, while strain measurement rosettes were installed in the vicinity of the web openings and on the beam-column joint). Sensors were sourced from Tokio Soki Kenkyjugo Co. Ltd. The same setup was adopted for all specimens, to ease comparision of results.

The focus of this research programme is on the post-yield behaviour of beams. Therefore, joint deformation must be minimised. For that purpose, stiffeners were placed at the beam-column interface, to prevent local buckling of the column flanges. Also, stiffeners were provided at the beam's end to prevent crushing of the beam's flange due to the concentrated load imposed by the actuator.

3.1. Test specimens

Four test specimens were evaluated in this research programme. Three have a web diameter of 233mm, equivalent to 0.8 times the depth between fillets; while the fifth one, RBW_1 has its flanges symmetrically trimmed according to guidelines in American Insitute of Steel Consruction AISC [1] at 180 mm from the column face. The first specimen, RWS_1, has a single web opening centred 180mm from the column face. The second, RWS_2 has periodical web openings along the entire beam spam, with a centerline spacing of 279mm except for the first web opening, which has a centre 180mm away from the column face. The third specimen has its first and second web openings centred at 300mm and 673mm away from the column face, while the spacing between sequent web openings was kept at 279mm onwards. An outline of all test specimens is depicted in Fig. 7. This is in accord with design guidelines considering vertical (gravity load) design of girders and flooring systems [17] and the results from numerical simulations conducted by [19,26]. The yield shear load of all specimens at the smallest cross-section is 149kN, which is larger than the largest valuable expected from the development of the full plastic mechanism or the beam considering plastification of the cross-section by a factor of 1.75 (the critical shear demand is two times the plastic moment divided by the span).

All structural elements were made in equivalent ASTM [2] A572 steel Grade 50 which has a nominal yield stress of 344N/mm^2. Material properties were verified by testing coupons extracted from the web and flanges of the specimens in accord with the ASTM [2] standard.

3.2. Loading protocol

Quasi-static cyclic testing was carried out in accord with the Federal Emergency Management Agency, FEMA [12] protocol. It is the standard way for prequalifying seismic connections [1]. A minor adjustment was done at the 0.01rad and 0.015rad deformation levels, as six cycles were imposed, instead of the 4 and 2 required by the standard. This was done to observe in detail the behaviour before yielding. The test protocol is depicted in Fig. 8.

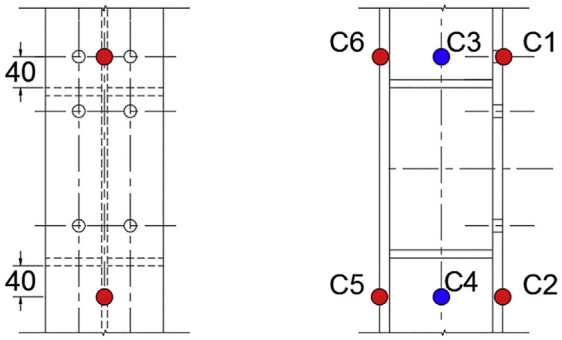

Fig. 5. Strain monitoring on the column. Uniaxial gauges are depicted on red, rosettes in blue.

4. Results

4.1. RWS_1

Incipient yielding started in the 29th load cycle after the measured stress in the uppermost fibre reached 358N/mm^2 (measured by strain gauge 1 in Fig. 4) at a beam chord rotation of 0.021rad. The moment associated with this rotation demand was 135.73kNm, which is 0.6 times the nominal capacity of the reduced cross-section. However, clear signs of yielding were not observed until a one and a half-cycle later, when slight surface crimping was observed on the edges of the web openings, at an angle between 10 and 20 degrees from the azimuth (web opening centreline), taken from a line going upwards from the centre of the perforation; along with appreciable elongation of the bolts at the bottom plate (Fig. 9).

As displacement demand increased, out-of-plane deformation became more prevalent, while there was no appreciable damage either in the column or within the panel zone joint. This indicates that single stiffeners corresponding to the beam flanges are enough to prevent buckling and tearing at this critical juncture.

Peak response was achieved in the last cycle (36th) for an imposed chord rotation of 0.051rad. The largest moments achieved were 206kNm and -203kNm respectively, this corresponds to 1.03 and 0.97 of the nominal moment capacity of the critical cross-section (Eq. (1)). At this stage, the shear on the critical cross-section was less than 50% of the yield shear load of the reduced section. Appreciable yielding was observed in the bottom flange, along with two opposing plastic hinges on the edges of the perforation at an azimuth of 23 degrees, in agreement with previous research [31, 32]. Therefore, there is evidence

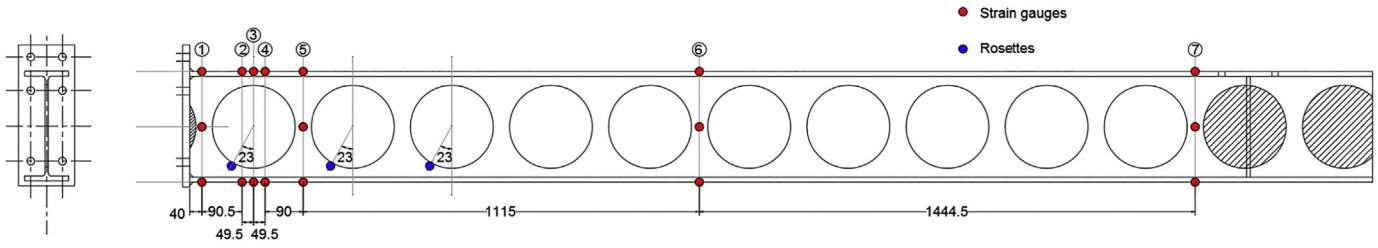

Fig. 4. Strain monitoring on the beam, uniaxial gauges are depicted on red, rosettes in blue.

Fig. 6. Strain gauge setup.

that a mixed mechanism involving both Vierendeel action and yielding of the cross-section occurred. The test was stopped due to extensive out-of-plane deformation, as observed in Fig. 10.

Inspection of the endplates once the test stopped showed extensive yielding of the studs along with plastic deformation around their holes. Likewise, there was appreciable prying of the endplate between the uppermost rows of bolts. Despite this there were no signs of incipient fracture, indicating that a sudden fragile failure was unlikely.

The hysteresis cycles described by moment-chord rotation plots (Fig. 11) indicate that the connection showcases an unsymmetric behaviour when the load moves upwards and downwards, along with extensive pinching. Despite this, the hysteresis cycles are symmetrical around a vertical line through the origin, indicating that the specimen does not tilt in a particular direction as the load is applied and reverses. Assessment of backbone curves during load reversals reveal that the slope of the moment-chord rotation relationship is 6354kNm/rad up to yielding. Then, the post-yielding stiffness, observed in the last test cycles, becomes 2850kNm/rad and 3094kNm/rad when the load goes up and down, respectively. Thus, there is an uneven reduction of 56% and 52%, demonstrating clearly how the backbone curves indicate that not only yielding thresholds are different, also the post-yield stiffnesses.

4.2. RWS_2

Yielding started in the 29th cycle when the chord rotation reached 0.02rad and the measured stress in the outermost fibre reached 367N/mm^2 when the specimen was subjected to a moment of 134kNm. In practical terms, it is the same threshold observed for RWS_1. However, immediate post-yield behaviour differs from what was observed in the previous case; as out-of-plane deformation and the Vierendeel mechanism manifested themselves right in the next cycle.

Peak response was recorded at 0.05rad, at the 36th cycle. While the negative moment capacity (tension the bottom fibre) reached 216kNm (5% larger than the nominal capacity) in opposite bending (tension in the upper fibre) reached only 176kNm 15% lower than the nominal capacity, while the maximum shear demand was less than 2/3of the yield value of the reduced cross-section. The most prevalent feature at this stage is the extensive lateral bending and buckling, which took the beam axis 23 degrees out-of-plane, along with extensive bucking of the bottom flange and the web section between the two web openings closest to the column face. Consequently, inelasticity spread out from the outermost perforation towards the beam's clear span (Fig. 12).

While inelastic action was limited in the panel zone, there was extensive yielding in the endplate. Prying was particularly noticeable between the top row of bolts, while there are appreciable elongation and bending of the bottom bolts (Fig. 13). Albeit extensive deformation of the endplate is undesirable, it must be remarked that ductile behaviour was predominant, instead of shearing or tearing, which would lead to a sudden loss of structural capacity.

The hysteresis cycles described by moment-chord rotation plots indicate that the connection showcases a highly skewed behaviour when the load moves upwards and downwards, along with pinching that appears less severe than what was observed for specimen RWS_1. However, the model does not tilt in a particular direction as the load reverses. Assessment of backbone curves taken from the hysteresis cycles (Fig. 14) during load reversals reveals that the slope of the moment-chord rotation relationship is 6044kNm/rad up to yielding. Then, the post-yielding stiffness, observed in the last test cycles, becomes 2092kNm/rad and 2450kNm/rad when the load goes up and down, respectively. Thus, there is a remarkable difference between post-yield slopes of the moment-chord rotation curves, as they are only 34% and 40% of the values before yielding.

4.3. RWS_3

The onset of yielding was observed during the 25th load cycle when a chord rotation of 0.01rad was imposed, leading to a measured stress of 357N/mm^2 at the topmost fibre. The recorded moment at this stage was 63kNm, 0.3 times the nominal moment resistance.

Yielding at the top flange, and incipient development of the Vierendeel mechanism was observed in the next cycles. Then, during the 30th load cycle, corresponding roughly to a rotation of 0.02rad, there was extensive inelastic deformation of the endplate, especially prying on the uppermost row of bolts during negative moment (load going down) along with yielding on the lower end of the plate during moment reversals. Likewise, bolts experienced observable elongation and buckling, without fracture. All these phenomena contributed to significant in-plane deformation at an early stage (Fig. 15).

Failure happened during the 35th load cycle when the weld joining the beam and its endplate tore. This occurred at an imposed chord rotation of 0.045rad, just after achieving peak moment values of 180kNm (negative) and 190kNm (positive), which are 0.86 and 0.90 times the nominal capacity, while the shear demand at the critical cross-section was only 52% of the yield value. There were no signs of inelastic deformation within the column, while a full collapse Vierendeel mechanism did not form within the beam (Fig. 16).

The hysteresis loops described in the chord-rotation moment diagrams depict extensive pinching, which is what is expected in cases where inelastic action clusters within the beam-column connection, as the behaviour is dominated by the slippage of bolts. Regardless of this, the specimen does not tilt in a particular direction as the load is reversed, as the hysteresis loops (Fig. 17) are centred around zero. The slope of the moment-chord rotation curves was 5713kNm/rad before yielding and averaged 3367kNm/rad (loading upward) and 3351kNm/

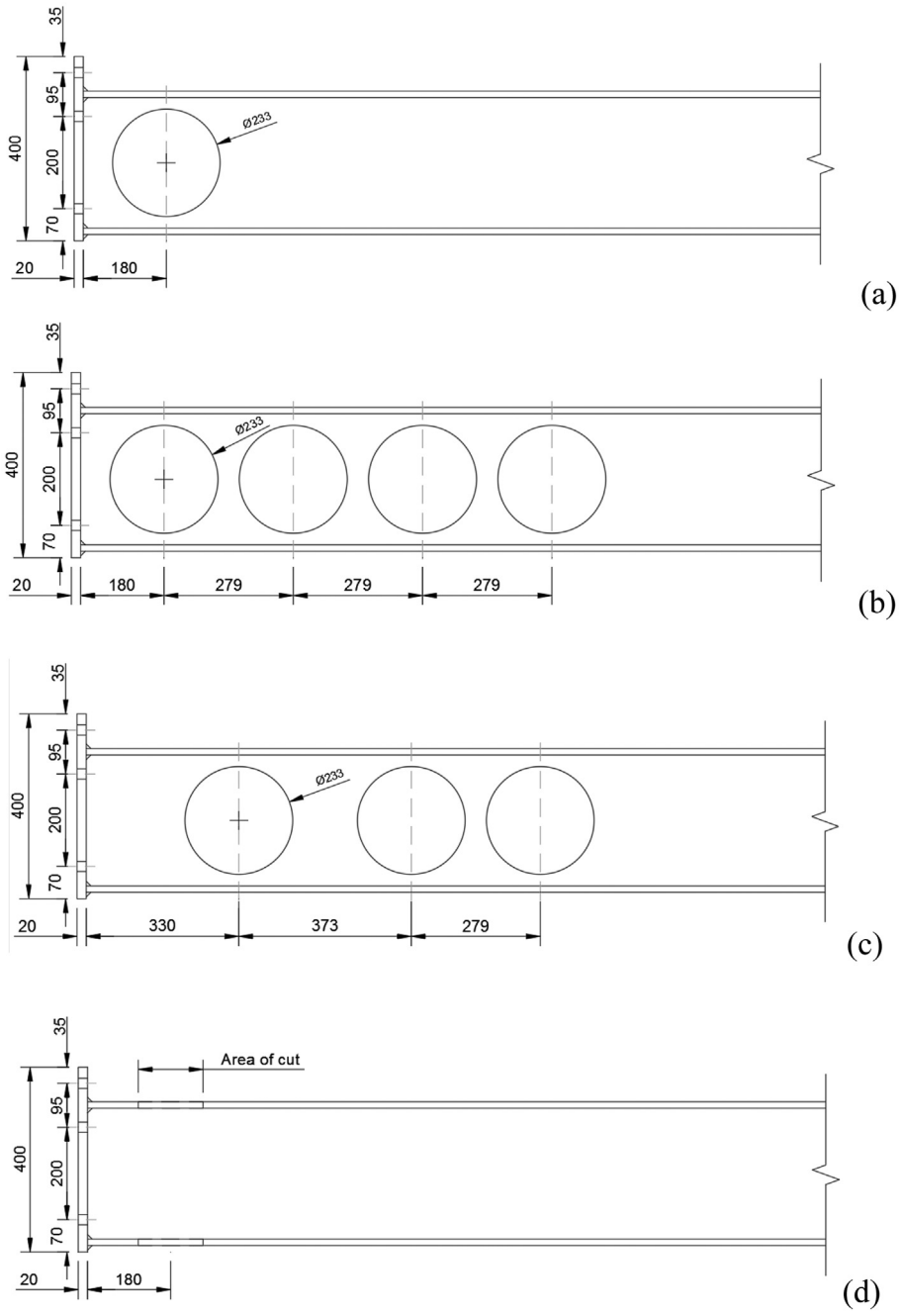

Fig. 7. Test specimens, RWS_1 (a), RWS_2 (b), RWS_3(c) and RBS_1 (d).

rad (loading downward) just right before failure; being in practical terms 0.59 times the value before yielding.

4.4. RBS_1

Yielding was observed after the 34th load cycle, at a rotation of 0.029rad when stresses in the uppermost fibre reached 357.59N/mm^2 while the moment applied was 123kNm, which is 0.62 times the nominal capacity (Eq. (3)). However, there was extensive yielding of the endplate connection at this stage, leading to an offset. Observable features of yielding within the protected zone were noticed until the 36th cycle, mainly surficial crimping and light bending of the reduced flange.

As cycles progressed, lateral bending and torsion built up, and more critically, the deformation of the endplate and the elongation of its bolts became even more noticeable, while the beam was responding elastically. This led to a separation of 7mm of the plate from the column face. Eventually, the test was stopped when a 0.04rad rotation was reached due to potential out-of-plane instability (Fig. 18). The recorded moment at this stage was 134kNm (negative) and 81kNm (positive), which is just 0.68 and 0.41 times the nominal capacity, respectively.

The hysteresis cycles (Fig. 19) described by the specimen are not all centred at the origin as there is plastic deformation in the plate before yielding within the beam. This leads to displacements that are not reversed as the load switches its direction, leading to a permanent offset. This also explains why a clear backbone curve is not depicted when the load reverses; it seems that the imposed displacement is not large

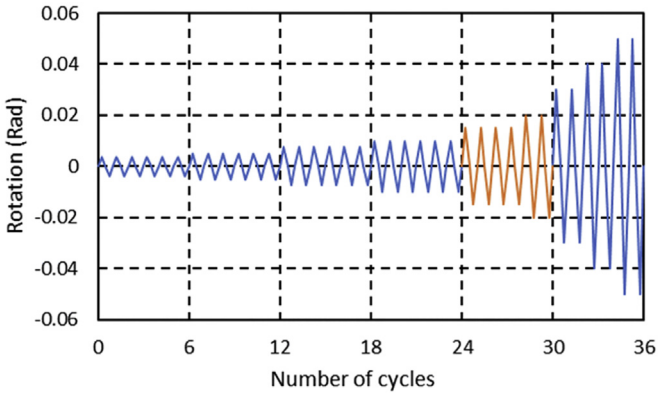

Fig. 8. Load protocol, adjustments made to the FEMA 350 protocol are highlighted.

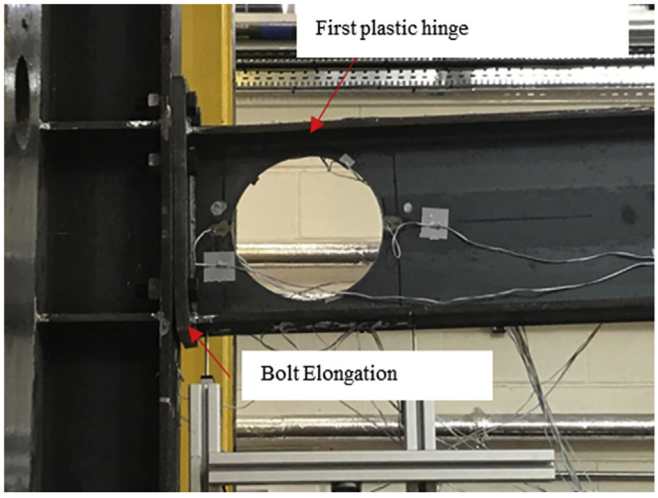

Fig. 9. Onset of yielding, RWS_1.

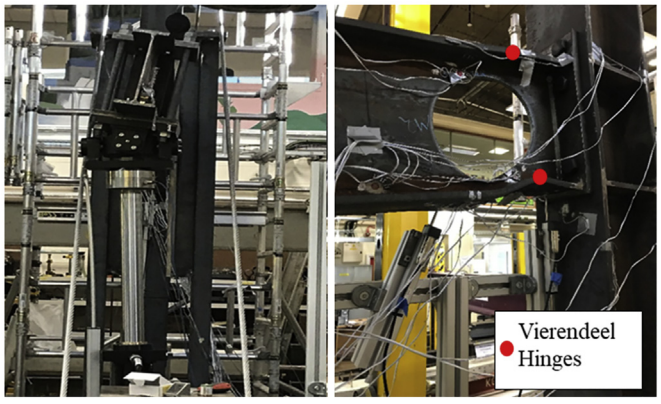

Fig. 10. Ultimate capacity RWS_1. Out of plane (left) and in-plane (right) deformation.

enough to properly reverse previous cumulative deformation completely, leading to the observed non-self-centring pinching.

4.5. Response benchmark considering the cruciform model

The testing scheme used in this study departs from the cruciform configuration (33), which is the most widespread benchmarking approach for assessing the seismic behaviour of beam-column

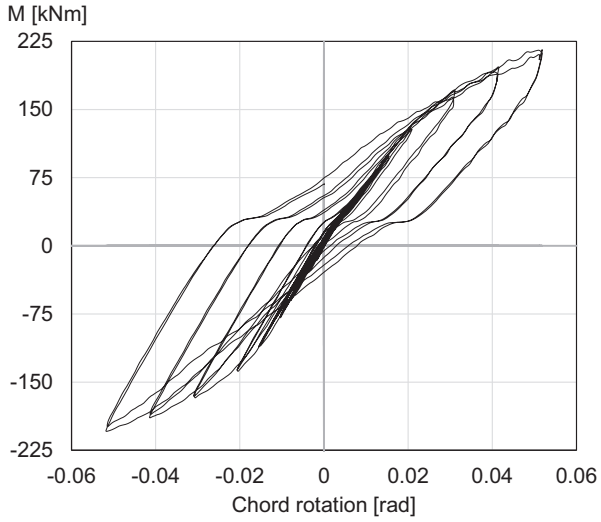

Fig. 11. Hysteresis cycles, RWS_1. M is the moment at the beam-column interface (including self-weight).

connections. [1]. However, expressions in the Annex, Eqs. (A.1)–(A.5) allow for estimation of equivalent deformation capacicity in terms of story drift demands (IDS) of a surrogate cruciform model. A summary of results is shown in Table 1.

All RWS connections display a capacity that greatly exceeds the minimum requirements for intermediate moment frames established by American Insitute of Steel Consruction AISC [1], as they can accommodate a story drift angle larger than 2% while achieving a moment capacity larger than 80% of the gross plastification moment of the reduced cross-section. This is a remarkable achievement taking into account that these connections were not designed in accordance with earthquake-resistant design specifications. Moreover, all RWS connections studied in this research programme achieved displacement ductilities close to or larger than 2, therefore it can be expected that a load reduction factor of at least 1.5 can be considered for preliminary seismic design of frames if the equal displacement rule is considered [7]. These assessments are yet preliminary, as full-scale tests considering the cruciform setup should also be carried out.

5. Discussion

Overall, RWS connections display stable moment-chord rotation hysteresis cycles without strength decay and one-sided permanent deformations. In all test specimens, yielding initiated in the vicinity of the web openings as expected, along with inelastic action in the topmost fibre of the critical section. A ductile behaviour was ensured in all cases until the test terminated due to extensive out-of-plane deformation. There was no evidence of fragile failure even for large deformation demands caused by chord rotations in excess of 0.04rad.

All RWS specimens were able to endure negative moments larger than the nominal capacity of the critical section; while exceeding 0.85 times the nominal capacity in the opposite direction. This indicates that the proposed connection can achieve yielding without subsequent strength degradation of sudden changes in stiffness, benefiting of the stable behaviour of the concurrent Vierendeel mechanism. The joint occurrence of both mechanisms limits inelastic deformation within the column and in the joint panel zone, as long stiffeners are provided behind the beam flanges, thus the 'strong-column weak-beam' concept has been realised. In all RWS specimens, there was yielding on the endplate and limited bending and buckling of its bolts, which explains pinching of the hysteresis cycles; firstly, bolts are strained in tension, then when the load reverses, they are compressed and buckle. Finally,

Fig. 12. Ultimate Capacity of RWS_2. In-plane deformation on left, out-of-plane on right.

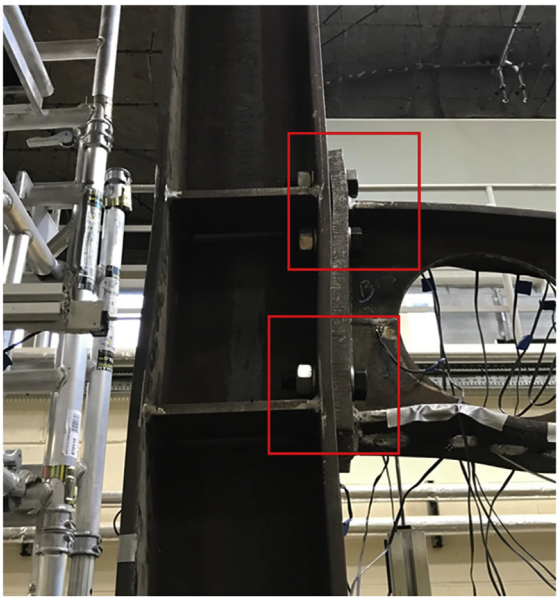

Fig. 13. Damage to the beam endplate at ultimate capacity, RWS_2.

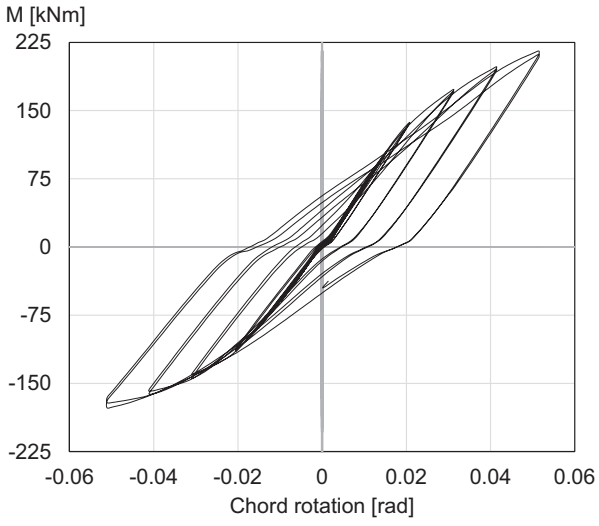

Fig. 14. Hysteresis cycles RWS_2.

a gap forms between the bolt and the plate. Before there is a proper restrain, that gap must be closed, making the connection behave in a manner akin to what is observed in a partially restrained connection [14].

Similarly, characteristics of the endplate could explain the unsymmetric behaviour on hysteresis cycles. The common practice in the UK is providing non-symmetrical top-extended endplates, as load reversals are considered unlikely. Thus, bending and buckling of bolts is more likely at the bottom end of the plate, as a single line of them is provided. This could have limited achieving the full nominal moment capacity of the beam when the load went upwards. This uneven distribution of bolts between bottom and top also makes lateral torsion and buckling more likely, as there is less restrain to out-of-plane actions, particularly when several openings are provided, as it was the case with specimens RWS_2 and RWS_3.

Performance of the connection diminishes if the first perforation is too far away from the column face. While specimens RWS_1 and RWS_2 were able to complete all 36 cycles without featuring a fragile failure mode, the RWS_3 specimen developed a fracture of a critical weld when a chord rotation of 0.045rad was imposed. It seems that the benefits of the Vierendeel mechanism were less than in the other cases and extensive demands were imposed on the connection, enough to lead to an unexpected tearing. Consequently, it is advisable to position the first perforation at a distance no larger than 1.5 times the diameter of the perforation to obtain the effects of the reduced web section, in accord with [26–28].

The behaviour of RWS beams, even when deployed using substandard characteristics for seismic design, among them the inclusion of unsymmetric endplates, was acceptable. No strength degradation was noticed, while limited stiffness degradation was observed. The slope of the moment-chord rotation curves was, even in worst conditions, at least 30% of the value before yielding. Pinching and undesired plastic behaviour within the endplates can be mitigated by providing an asymmetric array of bolts at its bottom and top ends, while properly designing them using capacity principles, to ensure that inelastic action is caused by the concurrent plastification of the critical cross-section and the Vierendeel mechanism.

Stain measurements on the top flange of all specimens validate assessments made. In all cases, strains are below 2%, which is far below typical values for the ultimate strain of structural steel, thus indicating that tearing is unlikely, and consequently, ample deformation capacity is still available.

Likewise, the effects of having several openings are also evident. For the first specimen, there is a steady build-up of strain, along with an observable permanent tension deformation, indicating that plasticity lumps on the single opening. Contrarily, peak strains in RWS_2 and RWS_3 are slightly less than one-quarter of this value, above the

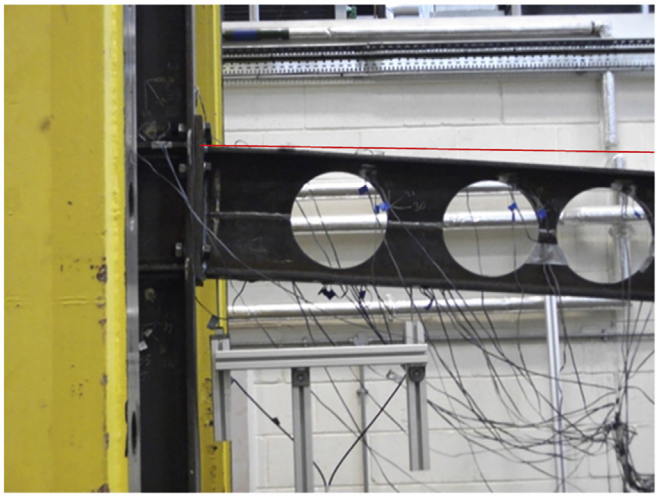

Fig. 15. Onset of yielding of RWS_4. The red line outlines the position before testing.

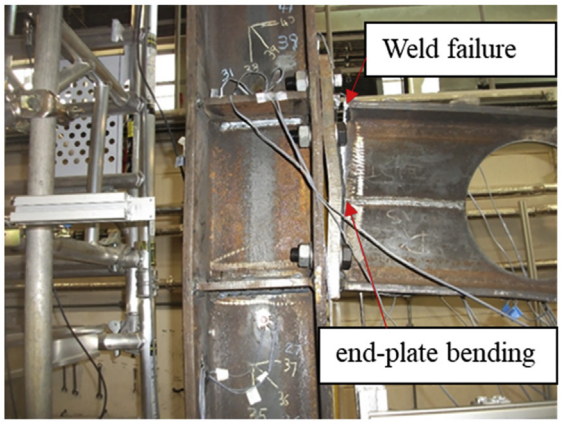

Fig. 16. Ultimate capacity RWS_4.

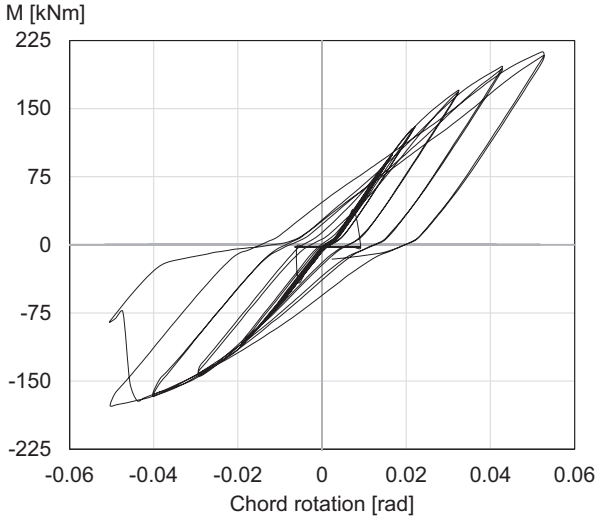

Fig. 17. Hysteresis cycles RWS_3.

yielding limit, but unlike what was observed for the first specimen, deformation only slightly builds up above this threshold, indicating that plasticity is likely to spread to other web openings (Fig. 20).

On other hand, the RBS comparable prototype connection underperforms when compared to what was observed for the RWS specimens. Even before yielding, there was extensive bolt bending and buckling, leading to large slippage in the endplate connection. Thus, a gap between the column face and the endplate formed, before yielding in the reduced section. Consequently, the hysteresis cycles were not centred around the origin, indicating that under cyclic actions shakedown could be critical [18]. Inelastic action within the endplate was more noticeable in the RBS specimen than in their RWS counterparts, probably due to less constrain to warping, buckling and torsion induced by the trimming of the flanges, indicating that connecting end plates play a larger role in the stability of RBS connections. This increased the deformation demands in the endplate, leading to the undesired behaviour observed.

6. Conclusions

This paper presents results of cyclic load tests on specimens representing frames in residential and front-end retail in the UK. Focus is on the response of frames with perforated (cellular) beams, which are becoming mainstream as they lead to larger clear spans while reducing self-weight and integrating building services.

However, the behaviour of bolted connections to cyclic actions was not explored experimentally before. Results of this research programme indicate that RWS connections can achieve their nominal moment capacity while describing stable hysteresis cycles without strength degradation. Moreover, RWS beam-column connections can achieve moderate ductility after yielding. Particularly, they can sustain storey drifts larger than 2% without showcasing fragile failure modes like tearing of flanges, webs, welds or joint panel zones, fracture of bolts or sudden buckling of endplates, as proper detail of protected zones is enforced. Therefore, they could be considered as moderate ductility connections, in accord with AISC guidelines.

This good performance originates in the concurrent yielding of the critical cross-section and development of Vierendeel moments on the edges of the web openings, in such way, that moment larger than 80% of the plastic moment of the cross-section can be achieved. Both phenomena lead to stable hysteresis cycles without strength degradation, while efficiently limiting inelastic behaviour within the column panel zone. Furthermore, post-yield slopes of moment-chord rotation curves are at least 30% of values observed before yielding.

It was found that stable response is highly influenced by proper detailing; the most critical factors are the separation of the first web opening from the column face and the proper capacity design of the beam endplates. Tests indicate that the distance between the first web opening and the column face should be less than 1.5 times the diameter of the web opening. On other hand, frames in the UK are not expected to experience a reversal of moments in beam-column connections. Therefore, it is common practice to provide a double layer or bolts solely at their top ends (either flush or extended endplate), while allocating a single line at the bottom. This is optimal for negative moments only. This leads to unsymmetric hysteresis cycles that showcase extensive pinching. It is possible that the behaviour of RWS connections can be remarkably improved by providing endplates with symmetric bolt arrangements, but this is beyond the scope of this study.

Results were further supported by assessing the behaviour of an RBS connection considering the same general underlying assumptions. The performance of the connection was notably lower than what it was observed for the RWS specimens. Less than half of the nominal capacity was achieved while the hysteresis cycles showed larger pinching and strength degradation. However, the least desirable trend noticed was the fact that the hysteresis cycles quickly wandered away from the origin, indicating that there was extensive inelastic action in the endplates

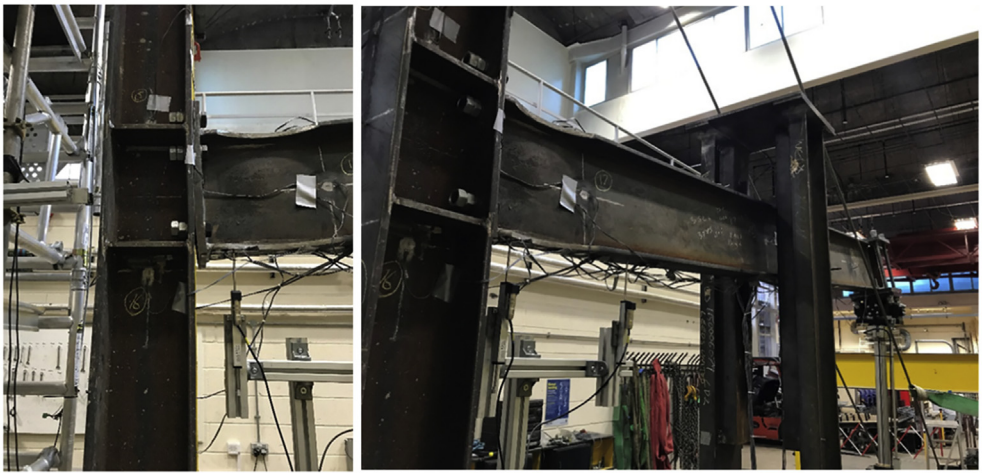

Fig. 18. Ultimate capacity, RBS_1. In-plane deformation (left), out-of-plane (right).

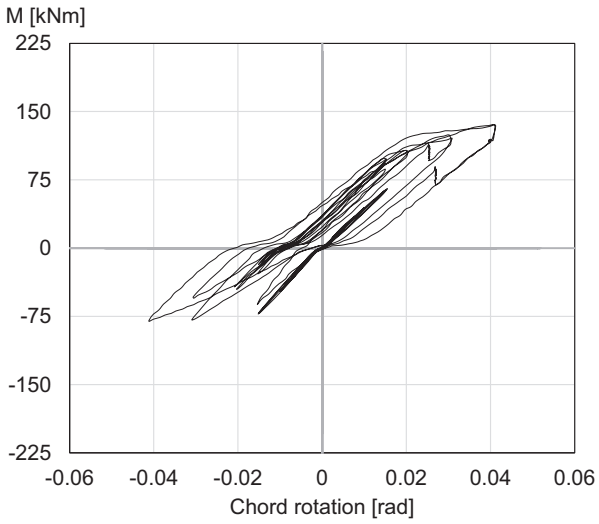

Fig. 19. Hysteretic behaviour RBS_1.

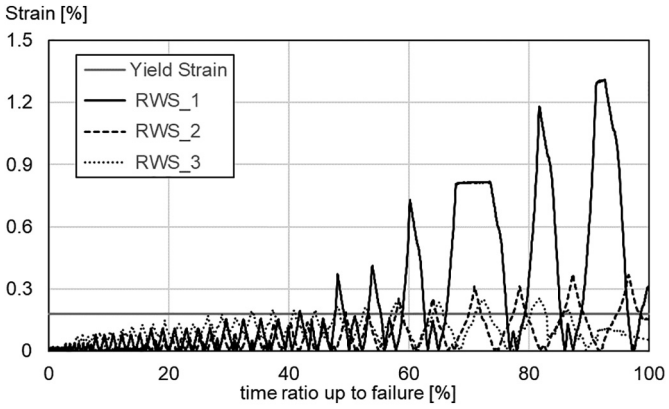

Fig. 20. Absolute value of strains on the top flange, above the first opening.

Table 1
Story-drift capacities of tested specimens, subscript y denotes yielding, u ultimate, μ_d is the displacement ductility.

Specimen	IDS_y [%]	IDS_u [%]	μ_d
RWS_1	1.5	3.3	2.25
RWS_2	1.7	3.5	1.98
RWS_3	0.7	2.2	2.94

even before the onset of yielding in the reduced cross-section, leading to skewed hysteresis cycles. Consequently, RBS beams without properly detailed endplates seem to be highly susceptible to shake-down.

Overall, RWS connections appear to be more resilient to unexpected cyclic actions, even when poor detailing for cyclic actions is provided. They appear to be capable of allowing for limited ductility. However, further studies of seismically designed RWS connections are required to validate if they can be considered as an alternative for seismic retrofitting of buildings. The results obtained in this study are promising, particularly demonstrating how RWS connections could be more suitable for seismic upgrading in regions were seismicity is sparse. Clearly, this study shows how optimisedallocation of material can reduce material consumption while keeping an acceptable structural performance. Moreover, it is the critical length opening, relevant to the position of the web opening along the length of the beam (as the angle of the plastic hinges is changing), and not the web opening area so much (i.e. weight reduction by one or more web openings) which predominately defines the capacity. Furthermore, typical sections studied followed basic circular web openings, thus, there is scope for further savings and potentially improved behaviour if optimisation procedures are employed.

Data availability

Videoshots of the RWS connections can be viewed here:
https://www.youtube.com/watch?v=Gx7zIRsyrFk
https://www.youtube.com/watch?v=WG14w_OncsU
https://www.youtube.com/watch?v=ZwEdT9W2Mkc
https://www.youtube.com/watch?v=TGCjOQGlAFQ

Authorship statement

All persons who meet authorship criteria are listed as authors, and all authors certify that they have participated sufficiently in the work to take public responsibility for the content, including participation in the concept, design, analysis, writing, or revision of the manuscript.

Furthermore, each author certifies that this material or similar material has not been and will not be submitted to or published in any other publication before its appearance in the Journal of Construction Steel Research.

Acknowledgments

The project is conducted with the support of the funders: Royal Academy of Engineering and The Leverhulme Trust (Grant number: LTSRF1819_15_40). The authors of this paper would also like to thank the University of Leeds for financially supporting the experimental campaign as well as Mr Farzad Neysari for offering technical expertise. Support for the third author was provided the IMAWARE initiative, which is funded by the Economic and Social Research Council of the UK (Grant number: ES/T003537/1).

Declaration of Competing Interest

We have no conflicts of interest to disclose.

Annex: Capacity assessment considering the proposed setup

According to the second-area moment theorem, the column end deflection of the proposed test setup is:

$$u_{ct} = \frac{M_b}{2}\left[\frac{H(H-h_b)}{2EI_c} + \frac{(H-h_b)^2}{4EI_c} + \frac{H}{Gt_{wc}h_b b_b}\right] \tag{A.1}$$

where u_{ct} is the top column displacement, M_b is the moment in the column, H is the setup modelled storey heigh, EI_c is the flexural stiffness of the column, h_b is the beam depth, h_c is the column depth, and G is the steel's shear modulus. Similarly, the elastic deflection of the tip of an equivalent beam without web openings (solid beam) would be given by:

$$u_{bt} = \frac{M_b}{2}\left[\frac{1}{2}\frac{(H-h_b)L}{EI_c} + \frac{L}{Gt_{wc}h_b b_c} + \frac{1}{6}\frac{(L-h_c)^2}{EI_b}\right] \tag{A.2}$$

The most widespread benchmark for assessing the seismic performance of connections is based on the cruciform arrangement, proposed by [33] which provides an estimate of story drift capacity. At yield, it takes the following value:

$$\theta_y = \frac{1}{12}\frac{M_b\left(1-\frac{h_c}{L}\right)}{\frac{EI_b}{L-h_c}} + \frac{(H-h_b)^2}{12EI_c}\frac{M_b}{H^2} + \frac{M_b}{H^2}\frac{(H-h_b)\left(\frac{H}{d_c}-1\right)}{Gt_{wc}h_c} \tag{A.3}$$

Then, it is possible to solve for both, column and beam flexural stiffnesses and then replace them in Eq. (A.3) to obtain estimates of storey drift, based on measurements collected with the proposed test setup.

Plastic displacement capacity observed in the test setup proposed in this study can be found directly by considering Eq. (3) as follows:

$$u_p = u_{lt} - M_u\left[\frac{1}{2}\frac{(H-h_b)L}{EI_c} + \frac{L}{Gt_{wc}h_b b_c} + \frac{1}{12}\frac{(L-h_c)^2}{EI_b}\right] \tag{A.4}$$

where u_p is the plastic rotation after discounting for joint rotation and column deformation, u_{lt} is the maximum beam displacement achieved, and M_u is the moment observed when u_{lt} is reached. Then, a lower bound estimate of the ultimate storey drift according to the cruciform model can be proposed, as follows:

$$\theta_u = \theta_y + \frac{u_p}{L} \tag{A.5}$$

References

[1] American Insitute of Steel Consruction AISC, Seismic Provisions for Structural Steel Buildings, 2016 (Chicago IL).
[2] American Society for Testing and Materials ASTM, Standard Test Methods for Tension Testing of Metallic Materials ASTM E8/E8M, 2016 West Conshohocken, PA.
[3] American Society of Civil Engineers ASCE, Specification for Structural Steel Beams with Web Openings SEI/ASCE 23–97, 1999 (Reston VA).
[4] M. Ascheim, Moment-Resistant Structure, Sustatiner and Method of Resisting Episodic Loads. US patent No 6012256, 2000.
[5] K. Boushehri, K.D. Tsavdaridis, G. Cai, Seismic behaviour of RWS moment connections to deep columns with European sections, J. Constr. Steel Res. 161 (2019) 416–435.
[6] S. Chao, S. Goel, Performance-based plastic design of special truss moments frames, Eng. J. AISC. 45 (2008) 127–150.
[7] A. Chopra, Dynamics of Structures, Prentice Hall, Upper Saddle River NJ, 2016.
[8] K.F. Chung, T.C.H. Liu, A.C.H. Ko, Steel beams with large web openings of various shapes and sizes: an empirical design method using a generalized moment-shear interaction, J. Constr. Steel Res. 59 (2003) 117–1200.
[9] S. Durif, A. Bouchair, Behavior of cellular beams ith sinusoidal openings, Proc. Eng. 40 (2012) 108–113.
[10] S. Erfani, A. Babazadeh, V. Akrami, The beneficial effects of beam web opening in seismic behavior of steel moment frames, Steel Compos. Struct. 13 (2012) 35–46.
[11] S. Fares, J. Coulson, D. Dinehart, Castellated and Cellular Beam Design. American Institute of Steel Construction, AISC, Chicaco IL, 2017.
[12] Federal Emergency Management Agency, FEMA, Recommended seismic design criteria for new steel-moment frame buildings, Report FEMA 350. Washington D. C, 2000.
[13] C. Gilton, C. Uang, Cyclic response and design recommendations of weak-axis reduced beam section moment connections, J. Struct. Eng. ASCE 128 (4) (2002) 452–463.
[14] T. Green, R. Leon, G. Rassati, Bidirectional tests on partially restrained, composite beam-to-column connections, J. Struct. Eng. ASCE. 130 (2) (2004) 32–327.
[15] L. Grilo, R. Fakury, A.L. Castro e Silva, G. Verissimo, Design procedure for the web-post buckling of steel cellular beams, J. Constr. Steel Res. 148 (2018) 525–541.
[16] A. Hedayat, M. Çelikağ, Reduced beam web (RBW) connections with circular openings, in: Lena M. Becker (Ed.), Structural Steel: Shapes and Standards, Properties and Applications, 2011 Nova Science Publishers 2011, Hauppauge, New York, 2011.
[17] R. Lawson, S. Hicks, Design of Composite Beams with Large Web Openings, The Steel Construction Institute, Berkshire UK, 2011.
[18] R. Leon, D. Flemming, Experimental verification of shakedown approaches for bridge design, Transp. Res. Rec. 1594 (1) (1997) 50–56.
[19] S. Momenzadeh, M. Kazemi, M. Hoseinzadeh, Seismic performance of reduced web section moment connections, Int. J. Steel Struct. 17 (2) (2017) 1–13.
[20] T. Montalbo, China, Global Warming and Hot-Rolled Steel Sections. Report F157-18, American Institute of Steel Construction, Chicago, IL, 2018.
[21] T. Moslehi, A. Deylami, Investigation of major parameters affecting instability of steel beams with RBS moment connections, Steel Compos. Struct. 6 (3) (2006) 203–219.
[22] S. Naimi, M. Celikag, A. Hedayat, Ductility enhancement of post-Northridge connections by multi longitudinal voids in the beam web, Sci. World J. Article 515936 (2013).
[23] J. Ruddy, S. Ioannides, Rules of thumb for steel design, Structures 2004: Building the past, Securing the Future. ASCE. Nashville TN, May 22-26, 2004.
[24] K.D. Tsavdaridis, Structural Performance of Perforated Steel Beams with Novel Web Openings and with Partial Concrete Encasement, Doctoral thesis City University London, 2010.
[25] K.D. Tsavdaridis, J.J. Kingman, V.V. Toropov, Application of structural topology optimisation to perforated steel beams, Comput. Struct. 158 (2015) 108–123.
[26] K.D. Tsavdaridis, C. Pilbin, C.K. Lau, FE parametric study of RWS/WUF-B moment connections with elliptically-based beam web openings under monotonic and cyclic loading, Int. J. Steel Struct. 17 (2017) 677–694.
[27] K. Tsavdaridis, T. Papadopoulos, A FE parametric study of RWS beam-to-column bolted connections with cellular beams, J. Constr. Steel Res. 116 (2016) 92–113.
[28] K.D. Tsavdaridis, F. Faghih, N. Nikitas, Assessment of perforated steel beam-to-column connections subjected to cyclic loading, J. Earthq. Eng. 18 (8) (2014) 1302–1325.
[29] K.D. Tsavdaridis, C. D'Mello, Finite element investigation of perforated beams with different web opening configurations, The 6th International Conference on Advances is Steel Structures (ICASS 2009). 16–18, December 2009, Hong Kong, China 2020, pp. 213–220.
[30] K.D. Tsavdaridis, C. D'Mello, Web buckling study of the behaviour and strength of perforated steel beams with different novel web opening shapes, J. Constr. Steel Res. 67 (10) (2011) 605–1620.
[31] K.D. Tsavdaridis, C. D'Mello, Optimisation of novel elliptically-based web opening shapes of perforated steel beams, J. Constr. Steel Res. 76 (2012) 39–53.
[32] Q. Yang, B. Li, N. Yang, Aseismic behaviors of steel moment resisting frames with opening in beam web, J. Constr. Steel Res. 65 (6) (June 2009) 1323–1336.
[33] A. Gupta, H. Krawinkler, Relating the Seismic Drift Demands of SMRFs to Element Deformation Demands," Engineering Journal, Am. Instit. Steel Construct. 39 (2002) 100–108.